# A Concerted Mechanism for the Suppression of a Folding Defect through Interactions with Chaperones

PROTEIN STRUCTURE AND FOLDING
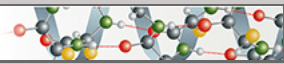
Shannon M. Doyle, Eric Anderson, Kristin N. Parent and Carolyn M. Teschke

Access the most updated version of this article at doi: 10.1074/jbc.M400467200

Find articles, minireviews, Reflections and Classics on similar topics on the JBC Affinity Sites.

Alerts:

- When this article is cited
- When a correction for this article is posted

Click here to choose from all of JBC's e-mail alerts

This article cites 49 references, 15 of which can be accessed free at
http://www.jbc.org/content/279/17/17473.full.html#ref-list-1

# A Concerted Mechanism for the Suppression of a Folding Defect through Interactions with Chaperones*

**Shannon M. Doyle, Eric Anderson, Kristin N. Parent, and Carolyn M. Teschke‡**

*From the Department of Molecular and Cell Biology, University of Connecticut, Storrs, Connecticut 06269-3125*

Specific amino acid substitutions confer a temperature-sensitive-folding (*tsf*) phenotype to bacteriophage P22 coat protein. Additional amino acid substitutions, called suppressor substitutions (*su*), relieve the *tsf* phenotype. These *su* substitutions are proposed to increase the efficiency of procapsid assembly, favoring correct folding over improper aggregation. Our recent studies indicate that the molecular chaperones GroEL/ES are more effectively recruited *in vivo* for the folding of *tsf:su* coat proteins than their *tsf* parents. Here, the *tsf:su* coat proteins are studied with *in vitro* equilibrium and kinetic techniques to establish a molecular basis for suppression. The *tsf:su* coat proteins were monomeric, as determined by velocity sedimentation analytical ultracentrifugation. The stability of the *tsf:su* coat proteins was ascertained by equilibrium urea titrations, which were best described by a three-state folding model, N ⇔ I ⇔ U. The *tsf:su* coat proteins either had stabilized native or intermediate states as compared with their *tsf* coat protein parents. The kinetics of the I ⇔ U transition showed a decrease in the rate of unfolding and a small increase in the rate of refolding, thereby increasing the population of the intermediate state. The increased intermediate population may be the reason the *tsf:su* coat proteins are aggregation-prone and likely enhances GroEL-ES interactions. The N ⇒ I unfolding rate was slower for the *tsf:su* proteins than their *tsf* coat parents, resulting in an increase in the native state population, which may allow more competent interactions with scaffolding protein, an assembly chaperone. Thus, the suppressor substitution likely improves folding *in vivo* through increased efficiency of coat protein-chaperone interactions.

The processes of protein folding and assembly are driven by the primary amino acid sequence (1, 2). Changes in this sequence, such as amino acid substitutions or deletions, can lead to protein misfolding and aggregation (3). These protein folding problems have been linked with serious human diseases (4–6). For example, a change in the amino acid sequence of the cystic fibrosis transmembrane receptor, most commonly ΔF508, causes misfolding and aggregation leading to cystic fibrosis (5, 7, 8). Osteogenesis imperfecta is caused by protein misfolding and is induced by many different amino acid substitutions that

weaken the collagen fibrils (4, 5, 9). The seriousness of these diseases highlights the significance of specific amino acids in the processes of protein folding and aggregation.

Our model system for studying the effects of amino acid substitutions on folding and assembly is coat protein of P22, a double stand DNA bacteriophage of *Salmonella typhimurium*. P22 coat protein is a 47-kDa polypeptide comprising 429 amino acids (10, 11). During assembly, 420 coat protein monomers and 150–300 molecules of scaffolding protein, an assembly chaperone, form a spherical procapsid into which DNA is packaged to form a phage (12–16). Single amino acid substitutions in the coat protein of P22 cause a temperature-sensitive-folding phenotype (*tsf*).[1] The *tsf* substitutions cause coat protein to aggregate *in vivo* when infected cells are grown at high temperature but are able to assemble into phage at low temperature (17, 18). At high temperatures, the folding of the *tsf* coat proteins is rescued by overproduction of the molecular chaperones GroEL and GroES *in vivo*, but WT coat protein folds independently of these chaperones (19, 20).

Our initial *in vitro* investigations of WT coat protein and *tsf* coat proteins determined how the *tsf* amino acid substitutions affect the folding and assembly of coat protein (21, 22). We found that coat protein has two folding domains defined by spectroscopic probes: a domain of secondary structure primarily monitored by circular dichroism (CD) and a hydrophobic domain with a tryptophan pocket, which can be monitored by tryptophan fluorescence. Coat proteins carrying the *tsf* substitutions A108V, G232D, and F353L all have decreased stability when compared with WT coat protein. In addition, the unfolding kinetics for the *tsf* coat proteins, monitored by fluorescence of the six tryptophans in coat protein (11), are ~8–14 times faster than the unfolding rate of WT coat protein. The most surprising result came from the kinetic experiments monitored by CD. Both the unfolding and refolding reactions of the *tsf* coat proteins are too fast to be monitored by manual mixing experiments (with a dead time of ~5–7 s), whereas WT coat protein had readily observable kinetics for both reactions (21). From our experiments, we concluded that the domain of secondary structure, which is monitored by CD, is "flickering" in and out of its native state and populating an intermediate. It is this flickering that makes the *tsf* coat proteins more aggregation-prone than WT coat protein and causes the *tsf* coat proteins to require GroEL and GroES for efficient folding *in vivo*.

Suppressor (*su*) substitutions were isolated at additional sites in coat protein to identify other amino acids that are important for folding or assembly (23). The isolated *su* substitutions result in a WT phenotype *in vivo*. Three second site suppressors, D163G, T166I, and F170L, were repeatedly iso-

‡ To whom correspondence should be addressed: Dept. of Molecular and Cell Biology, U-125, University of Connecticut, 91 N. Eagleville Rd., Storrs, CT 06269-3125. Tel.: 860-486-4282; Fax: 860-486-4331; E-mail: teschke@uconn.edu.

[1] The abbreviations used are: *tsf*, temperature-sensitive-folding; N, native state; I, intermediate state; U, unfolded state; *su*, suppressor; CD, circular dichroism; bisANS, 1,1′-bis(4-anilino)naphthalene-5,5′-disulfonic acid; WT, wild type.

lated from several different *tsf* coat protein mutants and are therefore referred to as global suppressors. Surprisingly, when purified *tsf:su* coat proteins were studied *in vitro*, we found that they were more aggregation-prone than their *tsf* parent coat proteins (24). However, with the addition of scaffolding protein, the phage assembly chaperone, to the *tsf:su* monomers, procapsid assembly can occur. The *tsf:su* coat proteins showed improved assembly rates and yields compared with the *tsf* parent coat proteins. From recent experiments,[2] we determined that the *tsf:su* proteins also had enhanced interactions with GroEL and GroES *in vivo*. Thus, we propose that the global suppressor substitutions rescue coat protein from the non-productive pathway of irreversible aggregation through a two-pronged mechanism *in vivo*: first through enhanced interactions with GroEL and GroES and second by increasing the rate of assembly of coat protein into a procapsid through interactions with scaffolding protein (24). Enhanced binding of the *tsf:su* coat proteins by GroEL and GroES might suggest that folding intermediates are either more populated or less stable. However, increased ability to assemble into procapsids indicates that the native state could be stabilized. Thus, our *in vivo* results present a puzzle: how can the folding of *tsf:su* coat proteins require enhanced interactions with GroEL and GroES and still have a stabilized native state for more efficient interactions with scaffolding protein?

Here, we examine the folding and stability of the *tsf:su* coat protein monomers *in vitro* to understand the molecular basis of the dual suppression mechanism. Using the *tsf* coat proteins S223F and F353L as well as these proteins with the global suppressor substitution T166I, we monitored changes in the folding rates and stability of the single and double substitution mutants. It appears that the T166I substitution may have differing effects on the stability of coat protein depending on the parent *tsf* substitution. Nevertheless, the T166I substitution appears to slow the folding and unfolding kinetics of the domain of secondary structure monitored by CD, as well as decreases the unfolding rate of the intermediate. Both changes in kinetics lead to an increased population of intermediate. Our data are consistent with our proposed hypothesis that the kinetic partitioning between aggregation and procapsids is regulated by the *su* substitutions. Moreover, the *tsf* and *tsf:su* substitutions in P22 coat protein highlight how particular amino acids in a protein sequence are crucial to proper folding and assembly.

## MATERIALS AND METHODS

*Chemicals, Buffers, and Proteins*—Ultrapure urea was purchased from ICN. All other chemicals were reagent grade and purchased from common sources. Purification of *tsf* and *tsf:su* coat protein mutants was done as previously described (14, 25–27). The final products of purification are empty procapsid shells, which are composed solely of coat protein. All experiments described below were done in 20 mM sodium phosphate buffer, pH 7.6.

*Unfolded and Refolded Coat Protein Monomers*—To obtain unfolded coat protein, empty procapsid shells were incubated in 6.75 M urea for 30 min at room temperature, which dissociates and denatures the subunits to monomers (21, 22, 25). Refolded coat protein monomers were formed by first denaturing empty procapsid shells in 6.75 M urea as described above. The unfolded coat protein was dialyzed overnight at 4 °C against phosphate buffer to remove the urea. The refolded coat protein monomers were held on ice until use.

*Velocity Sedimentation Analytical Ultracentrifugation*—The *tsf* and *tsf:su* coat protein samples, at about 1.0 mg/ml, prepared by microdialysis as described above, were diluted to 0.2 mg/ml and centrifuged in an AN-50Ti rotor pre-equilibrated at 20 °C. The solvent compartment was loaded with the dialysis buffer. The material was centrifuged at 50,000 rpm in a Beckman XLI AU and monitored with interference

optics until sedimentation of the boundary was complete. The analysis was done as previously described (22) using the programs Sednterp (28, 29) and Sedfit (30).

*Fluorescence and Circular Dichroism Measurements*—Fluorescence experiments were done with an SLM Aminco-Bowman 2 spectrofluorometer. The temperature of the cuvette was maintained at 20 °C with a circulating water bath. For equilibrium measurements, the excitation wavelength was 295 nm, and the emission wavelength was 340 nm, with both band-passes set to 4 nm. For kinetic measurements, an excitation wavelength of 295 nm, emission wavelength of 340 nm, and band-passes of 1 and 8 nm, respectively were used. Circular dichroism (CD) was done with an Applied Photophysics Pi-Star 180 spectropolarimeter with the cuvette maintained at 20 °C with a circulating water bath. The CD signal was monitored at 222 nm with a slit width of 4 nm for equilibrium and kinetic experiments. A 1-cm path-length cell was used for equilibrium titrations and kinetic experiments. Equilibrium measurements in the CD and fluorometer were averaged for 30 s per sample.

*Unfolding and Refolding to Equilibrium*—Samples for urea equilibrium titration curves were made using a Hamilton Microlab 500 titrator as described previously (21, 22). Approximately 70 samples were used for each technique to define the equilibrium curves. The equilibrium transitions were monitored by tryptophan fluorescence and CD as described above. Data analysis was done as previously described, using the program Savuka (21, 22), except least-square errors are reported rather than the errors from the robust analysis. The $\Delta G^0(H_2O)$ and the sensitivity of each transition to denaturant, *m*, were determined by fitting the equilibrium data sets assuming a linear relationship between the free energy of unfolding for each transition and the denaturant (31, 32). For the global fit, all of the data from each technique were analyzed simultaneously, and the thermodynamic parameters were obtained as described in Finn *et al.* (31) using the formula,

$$F_{signal} = K_{NI}(Z_I + K_{IU})/[1 + K_{NI}(1 + K_{IU})] \qquad \text{(Eq. 1)}$$

where $K_{NI} = [I]/[N]$ and $K_{IU} = [U]/[I]$ and $Z_I = (Y_I - Y_N)/(Y_U - Y_N)$. The *Z*-parameter normalizes the optical properties (*Y*) of the intermediate to that of the native and unfolded states. The *Y* values were treated as local parameters, whereas the $\Delta G^0(H_2O)$, and the *m* values were globally fit. The *Z* value was allowed to vary between the fluorescence curve and the CD curve, so that two *Z* values were determined for each fit. A *Z* value of 0 means the intermediate has native-like spectroscopic properties, and a *Z* value of 1 means the intermediate is like the unfolded state. Initial fitting estimates of the native and unfolded baseline slopes for the *tsf* mutants were based on the slopes from the fit of the equilibrium data for WT coat protein (21). The native baseline slopes for the equilibrium curves monitored by CD for each *tsf:su* coat protein and their *tsf* parent were set to be similar. The fraction of each species at different urea concentrations was calculated using the equilibrium parameters for each transition from the three-state fit, again using the program Savuka (33, 34).

*bisANS Binding Assay*—bisANS binding to WT and *tsf* coat proteins was determined using a double titration method with the excitation wavelength set at 400 nm and the emission wavelength at 490 nm (35, 36). In one titration the bisANS concentration is fixed and the concentration of coat protein is varied. The *y*-intercept of a plot of $1/F$ *versus* $1/[\text{coat}]$ is $1/F_{max}$, where $F_{max}$ is the maximum fluorescence intensity. $F_{max}/[\text{bisANS}]$ is the maximum fluorescence units/$\mu$M bisANS bound to coat protein. In the second titration, the coat protein concentration was held at 0.5 $\mu$M, and the bisANS concentration varied from 0.5 to 50 $\mu$M. The fluorescence of both background and sample was corrected for the inner filter effect, which becomes substantial at high [bisANS], as described by Lakowicz (37). The fluorescence values were converted into $\mu$M bisANS bound/$\mu$M coat protein. A plot of $\mu$M bisANS bound/$\mu$M coat protein *versus* free [bisANS] was analyzed with KaleidaGraph (Synergy Software) using the formula $y = n[\text{bisANS}]/(K_d + [\text{bisANS}])$, where *n* is the number of sites and $K_d$ is the dissociation constant (35). The bisANS binding isotherm of WT coat protein, and for one of the *tsf:su* coat proteins, showed positive cooperativity, and therefore was analyzed with the Hill equation, $\log F/F_{max} = n \log[\text{bisANS}] - \log K_d$ (38). At least three data sets were averaged for the values given in Table II.

*Kinetics of Unfolding and Refolding*—Unfolding experiments were done with coat protein monomers prepared as described above at a final protein concentration of 0.4 $\mu$M. To initiate an unfolding reaction, the *tsf* coat protein monomers were diluted 1:50 with buffered urea. Refolding experiments were done with coat protein that had been denatured in 6.75 M urea. To initiate refolding, unfolded coat protein was diluted 1:100 with buffered urea solutions (0.4 $\mu$M final protein concentration).

The constantly stirred reactions were monitored by fluorescence. The final urea concentration was determined by measuring the refractive index. Kinetic experiments monitored by CD at 222 nm were done as described above, but with a final protein concentration of 2 $\mu$M monomer. The kinetic traces were fit with two exponentials as described previously to obtain a relaxation time for each experiment (21, 22). The log of the relaxation times from the kinetic experiments was plotted in a chevron plot against the urea concentration. The urea dependence of the slow refolding and unfolding relaxation times, when monitored by tryptophan fluorescence, was fit with an equation for a two-state system modified from Ghaemmaghami *et al.* (39), as previously described (21, 22). From this analysis, the $\tau_f$ and $\tau_u$ ($1/k_f^\circ$ and $1/k_u^\circ$, respectively), which are the folding and unfolding relaxation times in the absence of urea; the $m_{eq}$ and $\alpha$ are determined. The $m_{eq} = RT(m_u^\ddagger - m_f^\ddagger)$, where $m_u^\ddagger$ and $m_f^\ddagger$ are the slopes of the unfolding or refolding arms of the chevron plot and reflect the sensitivity of each reaction to denaturant. The $m_{eq}$ is similar to the $m$ value obtained from equilibrium urea titrations. $\alpha = (m_u^\ddagger/m_u^\ddagger - m_f^\ddagger)$ and is a measure of how similar the transition state of the reaction is to the native state or the unfolded state. When $\alpha$ is close to 1, the position of the transition state is near the native state, and if $\alpha$ is close to 0, the transition state is near the unfolded state (40). The errors presented are the standard deviation values from the fitting of the equation using KaleidaGraph (Synergy Software).

## RESULTS

In an earlier study, we determined that *tsf* substitutions in coat protein lead to a destabilized native state and a highly populated intermediate state (22). This destabilization is caused by a rapid flickering between the native and unfolded states of a domain of secondary structure of coat protein, as well as an increased rate of unfolding of a hydrophobic tryptophan pocket. Here, we determine how the *su* substitutions modify the folding of the original *tsf* substitution. We have chosen S223F and S223F:T166I as well as F353L and F353L:T166I coat proteins for this study. In our previous experiments we used the T166I substitution, because it was the most frequently isolated global suppressor (24). Moreover, S223F and F353L were the parents that most often isolated the global suppressors.

*tsf Parent and Suppressor Coat Proteins Fold into Monomers*—We previously reported that WT coat protein and *tsf* coat proteins with single amino acid substitutions are monomeric when refolded from denaturant. Under identical conditions (22), we studied the oligomeric state of S223F:T166I and F353L:T166I substitution mutants, as well as their parent *tsf* coat proteins using velocity sedimentation analytical ultracentrifugation. The velocity sedimentation data were analyzed using the program Sedfit (30). Using the c(s) method for sedimentation analysis, the $s_{20,w}$ values for S223F, S223F:T166I, and F353L:T166I coat proteins were determined to be 3.6, 3.2, and 3.6, respectively. The previously published values for WT, A108V, G232D, and F353L coat proteins are 3.4, 3.3, 3.3, and 3.6, respectively (21, 22). These values are consistent for proteins with a molecular mass of 47 kDa and varying asymmetries. Additionally, the percentage of higher molecular weight species was between 4 and 19%, which is similar to that observed for WT coat protein and the previously studied *tsf* coat proteins. From these results, we can conclude that the *tsf:su* coat proteins fold into monomers, as do the WT and *tsf* coat proteins.

*The Stability of the tsf:su Proteins*—The thermodynamics of folding for WT coat protein, as well as coat proteins with *tsf* amino acid substitutions have been previously studied (21, 22). For both WT coat protein and the *tsf* coat proteins, the equilibrium folding data were fit to a three-state model (N $\Leftrightarrow$ I $\Leftrightarrow$ U) (21, 22, 34). In these experiments, we found that the *tsf* coat proteins are less stable than WT coat protein, especially in the N $\Leftrightarrow$ I transition.

Equilibrium urea titrations were done to determine the sta-

bility of the *tsf:su* coat proteins. The equilibrium transitions for the coat protein variants were monitored using both intrinsic tryptophan fluorescence with an emission wavelength of 340 nm and circular dichroism (CD) at 222 nm. These wavelengths were chosen to maximize the difference in signal between folded (0 M urea) and unfolded (4 M urea) coat protein. This translated into a ~30% decrease in fluorescence signal between folded and unfolded protein monitored at 340 nm, and a decrease in signal for CD at 222 nm of ~ 75%. In previous studies, we established the reversibility of coat protein folding and unfolding (21, 22). Also, unfolded coat proteins refold into monomers, and in the presence of scaffolding protein these monomers are assembly-competent, again demonstrating that coat protein monomers can be reversibly folded (21, 22, 24).[2]

As observed before, the transitions for the CD and tryptophan fluorescence were not coincident, indicating that the folding of the *tsf:su* coat proteins was not a two-state process. From our studies of the folding of WT and *tsf* coat proteins, we know that CD at 222 nm primarily monitors the N $\Leftrightarrow$ I transition, whereas tryptophan fluorescence primarily monitors the I $\Leftrightarrow$ U transition. The data for S223F:T166I and F353L:T166I coat proteins were again best described using the three-state model, N $\Leftrightarrow$ I $\Leftrightarrow$ U (Figs. 1 and 2), and the lines are the fit of the data to that model. These data were not well described with a two-state model. Even using a three-state model these data were difficult to fit, because the native CD baselines are not well defined, although this fit was much improved over the two-state fit. The baselines were established as described under "Material and Methods." The large errors for the thermodynamic parameters determined by the three-state fits of the *tsf:su* coat proteins reflect the difficulty in fitting these data. The fits presented here are the best fits we were able to attain as indicated by the reduced $\chi^2$ values. We fit the F353L data again, using the methods described under "Materials and Methods" to establish the baselines and returned values within error of those determined previously (22) (Table I). These new fits are shown here (Figs. 1 and 2). Both S223F and F353L were fit equally well with either a two-state or three-state equilibrium model with reduced $\chi^2$ values that were not significantly different. We have chosen to present here the fits of the three-state model, because the kinetics of folding and unfolding remain consistent with a three-state model (see below).

Both S223F and F353L coat proteins showed a significant destabilization compared with WT coat protein over the first transition (N $\Leftrightarrow$ I), but less of a change in stability over the second transition (I $\Leftrightarrow$ U) (Table I). The change in solvent accessibility (*m* value) for the first transition was much smaller for the *tsf* mutant coat proteins than for WT coat protein, whereas the *m* values for the second transition were similar to WT coat protein. These results are consistent with our earlier work with other *tsf* coat proteins (22).

The suppressor substitution, T166I, had a different affect on the stability of the two *tsf* coat proteins (Figs. 1 and 2). The stability of F353L:T166I coat protein for the N $\Leftrightarrow$ I transition was not altered by the addition of the suppressor substitution, whereas the second transition increased in stability by ~1.1 kcal/mol, an increase of greater than 50% (Table I). The change in solvent accessibility of the F353L:T166I coat protein for the N $\Leftrightarrow$ I transition was within error as compared with the F353L. The *m* value for F353L:T166I coat protein over the I $\Leftrightarrow$ U transition was not significantly different than either F353L or WT coat proteins. On the other hand, the addition of the T166I suppressor substitution to the S223F *tsf* mutant coat protein caused the *tsf:su* coat protein to have an increase in both stability and *m* value for the N $\Leftrightarrow$ I transition over that of the S223F coat protein. Little change in stability and *m* value for
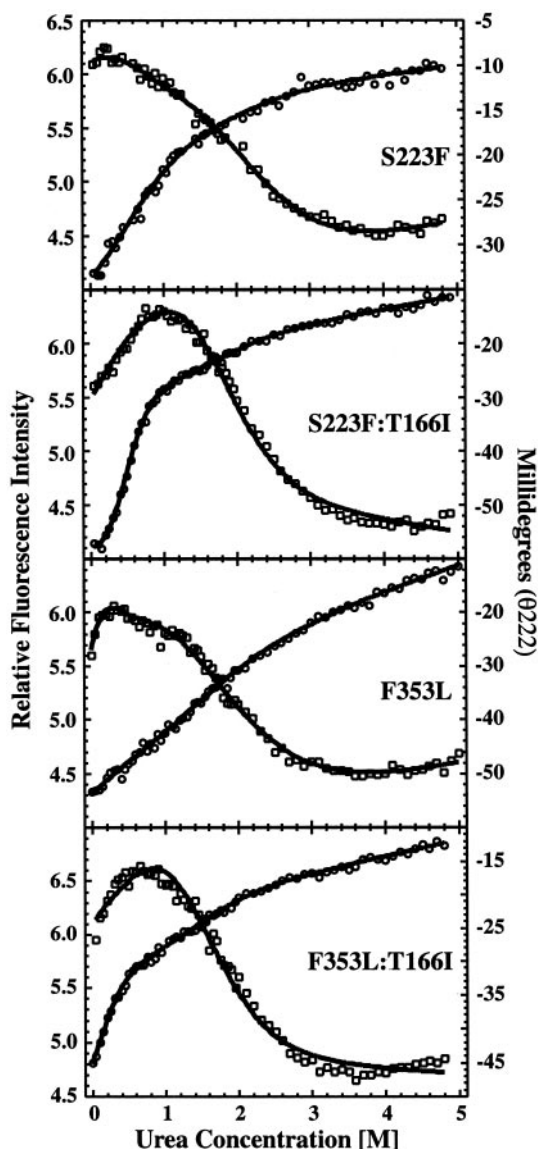
FIG. 1. **Equilibrium folding transitions of the *tsf:su* coat proteins and the *tsf* coat protein parents monitored by tryptophan fluorescence and circular dichroism.** Each of the *tsf* and *tsf:su* coat proteins was incubated at 2 $\mu$M (100 $\mu$g/ml) in solutions containing various urea concentrations at 20 °C. The fluorescence was measured with the excitation at 295 nm and the emission at 340 nm (□). The ellipticity was monitored at 222 nm (○). The *lines* are the global fit of all the data to a three-state model as described under "Materials and Methods." The thermodynamic parameters determined from the fits are shown in Table I.

the I ⇔ U transition was observed for the S223F:T166I coat protein. Although there is an increase in stability for the N ⇔ I transition, there remains an over 60% decrease in stability compared with WT coat protein. In all cases the *Z*-parameters are not well enough defined to evaluate the effect of the T166I substitution on the optical properties of the intermediate. Thus, the addition of T166I to F353L does not alter the stability of the native state, whereas its addition to S223F increases the native state stability.

Fraction of species plots were generated from the thermodynamic parameters of the three-state fit to more easily compare changes in the populations of native, intermediate, and unfolded species (Fig. 2). The folding intermediate (*dotted line*) was easily visible with a maximum population at urea concentrations between 0.4 and 1 M comprising between 60 and 85% of the species present. The low stability of the first transition for
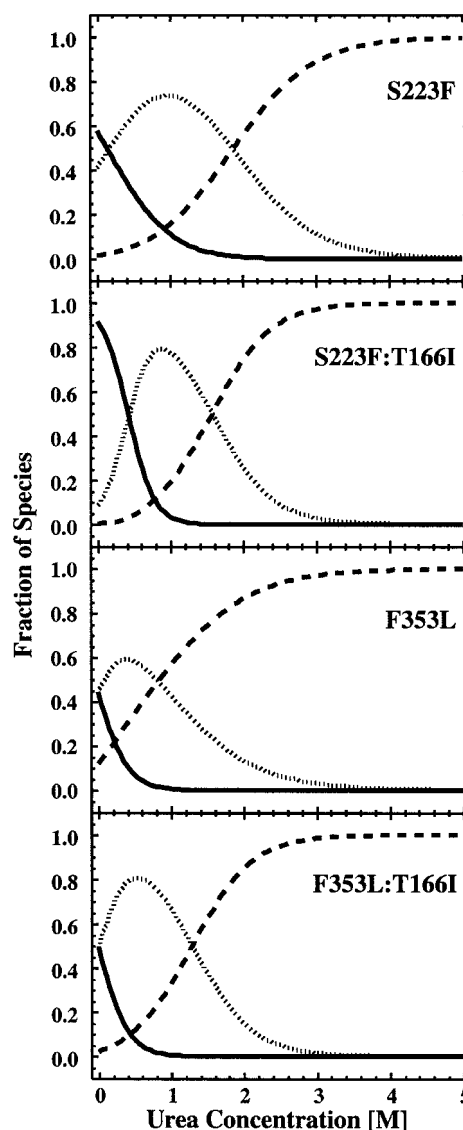


FIG. 2. **Fraction of species at different urea concentrations.** The equilibrium constants and *m* values determined from the global analysis of the equilibrium folding data (Table I) were used to determine the fraction of the native state (*solid line*), the folding intermediate (*dotted line*), and the unfolded protein (*dashed line*) at various urea concentrations.

S223F coat protein was apparent, because the intermediate state is already 40% populated in 0 M urea, whereas the native state for the S223F:T166I coat protein was 90% populated in 0 M urea. The one striking difference between the F353L and the F353L:T166I coat proteins was that the intermediate of the *tsf:su* coat protein is more populated, indicating that it is stabilized.

*The tsf:su Coat Proteins Show Differential Binding of bisANS*—The results of our equilibrium titrations indicated that the T166I substitution has a different effect depending on the *tsf* parent. The native state of S223F is stabilized, whereas it is the intermediate of F353L that is stabilized by the addition of T166I. To confirm this result, we studied the binding of the hydrophobic dye bisANS, a probe for exposed hydrophobic patches on proteins (41). From previous experiments we know that the *tsf* coat proteins, A108V, G232D, and F353L, have a higher affinity for, and bind significantly more, of the hydrophobic dye bisANS than does WT coat protein, indicating a general increase in surface hydrophobicity (25). In addition, no positive cooperativity in binding bisANS is observed for the *tsf*

TABLE I

*Thermodynamic parameters determined from global analysis of equilibrium urea titrations*

Data were fit globally to a three-state model, N ⇔ I ⇔ U. Fluorescence (FL) and CD fits were performed on data collected at 2 $\mu$M monomer.

| Coat Protein | $\Delta G^0$ (NI) | $\sim\Delta\Delta G^0$ (NI) | -m (NI) | $\Delta G^0$ (IU) | $\sim\Delta\Delta G^0$ (IU) | -m (IU) | Z-parameter | |
|---|---|---|---|---|---|---|---|---|
| | | | | | | | FL | CD |
| | *kcal/mol* | *kcal/mol* | *kcal/mol/M* | *kcal/mol* | *kcal/mol* | *kcal/mol/M* | | |
| WT[a] | $-3.69 \pm 0.26$ | | $5.44 \pm 0.44$ | $-2.09 \pm 0.30$ | | $1.28 \pm 0.12$ | $0.05 \pm 0.01$ | $0.76 \pm 0.08$ |
| S223F | $-0.20 \pm 0.018$ | 3.5 | $1.30 \pm 0.05$ | $-1.96 \pm 0.49$ | 0.1 | $1.05 \pm 0.13$ | $0.67 \pm 0.06$ | $0.91 \pm 0.03$ |
| S223F:T166I | $-1.39 \pm 0.25$ | 2.3 | $3.23 \pm 0.23$ | $-2.24 \pm 0.59$ | $-0.2$ | $1.43 \pm 0.27$ | $0.08 \pm 0.75$ | $0.88 \pm 0.05$ |
| F353L | $-0.005 \pm 0.75$ | 3.6 | $2.49 \pm 1.54$ | $-0.76 \pm 0.99$ | 1.3 | $0.92 \pm 0.20$ | $0.70 \pm 0.32$ | $0.35 \pm 0.44$ |
| F353L:T166I | $-0.0002 \pm 0.23$ | 3.7 | $2.77 \pm 0.41$ | $-1.83 \pm 0.48$ | 0.3 | $0.1.42 \pm 0.22$ | $0.34 \pm 0.76$ | $0.83 \pm 0.06$ |

[a] Data taken from Anderson and Teschke (21).

coat proteins, but cooperativity is seen for WT coat protein (25). To confirm changes in the native state of the *tsf:su* coat proteins, we investigated the binding of bisANS to WT, S223F, F353L, S223F:T166I, and F353L:T166I coat proteins using Scatchard or Hill analysis (Fig. 3 and Table II). The *tsf* coat proteins, S223F and F353L, follow the same pattern as the other *tsf* coat proteins, having no cooperativity in binding and a higher affinity for bisANS than WT coat protein. The *tsf:su* coat protein, S223F:T166I, had a binding isotherm that showed positive cooperativity and yielded a Hill coefficient similar to that of WT coat protein (Fig. 3), indicating a change in the tertiary structure of this coat protein that alters the amount of exposed hydrophobic surface area to a more compact structure, similar to WT coat protein. Using Hill analysis led to a significant improvement in the $\chi^2$. Conversely, F353L:T166I had a $K_d$ similar to that of its *tsf* parent. Thus, the binding of bisANS confirms that T166I substitution causes the native state of S223F to become more like WT coat protein, whereas it has little affect on the native state of F353L.

*The Rate of Flickering of the Secondary Structure Decreases in the Presence of the Suppressor Substitution*—The *tsf* coat proteins studied in Doyle *et al.* (22) have unfolding and refolding kinetics that occur too rapidly to be monitored by CD. This rapid flickering of the N ⇔ I transition caused the instability and the propensity to aggregate of the *tsf* coat proteins (22). Because the T166I substitution appears to have different affects on the stability of the *tsf* coat proteins, an overall stabilization of the native state does not seem to be the mechanism by which the *su* substitution functions. Therefore, we investigated whether the addition of the suppressor substitution would slow down the kinetics of refolding and unfolding monitored by CD as a means of suppression of the *tsf* phenotype.

When the kinetics of the *tsf:su* mutant coat proteins were monitored by CD, unfolding kinetics could be seen for both S223F:T166I and F353L:T166I coat proteins. We were unable to fit the unfolding kinetics for F353L:T166I coat protein as they were too rapid and the amplitude small, but unlike F353L coat protein, kinetics were discernible. In the presence of the suppressor substitution, refolding kinetics were also evident for S223F:T166I coat protein, but not for F353L:T166I. The *tsf* mutant, S223F, was different than the other *tsf* mutant coat proteins. S223F showed observable refolding CD kinetics, although like other *tsf* mutants, the unfolding reaction was too rapid to be observed. The kinetic data for both S223F and S223F:T166I coat proteins were best fit to a first order reaction with two exponentials, as established for WT coat protein (21). Because S223F:T166I coat protein had both observable unfolding and refolding kinetics, the relaxation times were plotted *versus* the urea concentration in a chevron plot (Fig. 4). The relaxation times for the folding reactions of S223F are also shown in the chevron plot. These showed an unusual increase in the rate of folding as the denaturant concentration increased (Fig. 4). The fit of the data for WT coat protein is shown for comparison (21). The chevron plot data for S223F:T166I coat
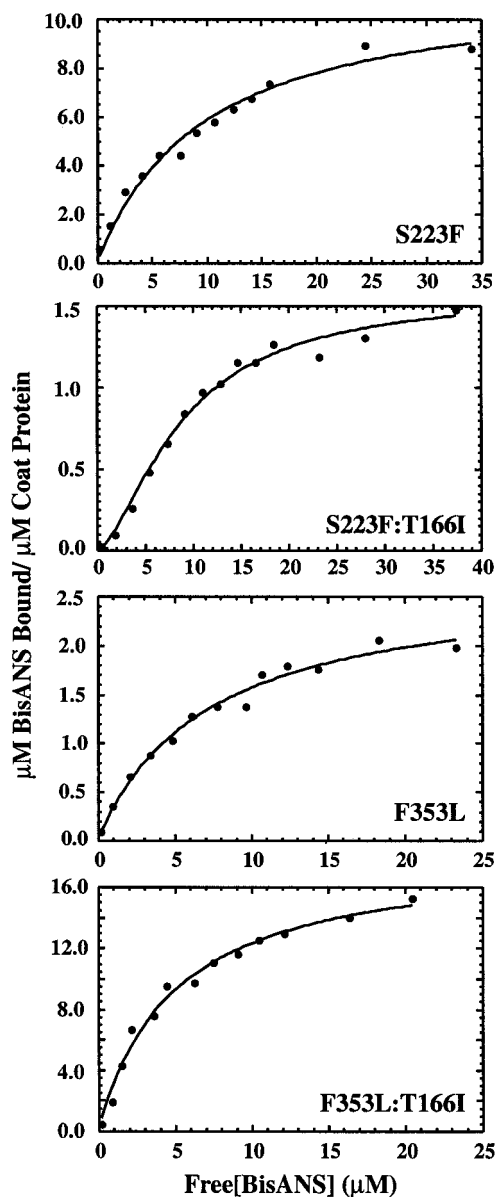


FIG. 3. **BisANS binding to the native *tsf* and *tsf:su* coat proteins.** The affinity of bisANS for coat protein was determined using the double titration method, as described under "Materials and Methods." S223F, F353L and F353L:T166I were able to be fit using Scatchard analysis, whereas S223F:T166I required Hill analysis for cooperative binding (25, 35). The data shown are representative of many sets. The *lines* are the fit of the data to either the Scatchard equation or the Hill equation.

protein were fit as described above, and the parameters for that fit are in Table III. The thermodynamic parameters determined from the kinetic experiments were similar to those de-

TABLE II
*Binding of bisANS to WT, tsf, and tsf:su coat proteins*

|  | $K_d$ | Number of sites | Hill coefficient |
|---|---|---|---|
|  | μM |  |  |
| WT[a] | 74.5 ± 19.8 |  | 1.1 ± 0.1 |
| S223F | 9.8 ± 5.8 | 12.0 ± 1.0 |  |
| S223F:T166I | 40.0 ± 14.3 |  | 1.1 ± 0.4 |
| F353L[a] | 9.7 ± 2.3 | 8.3 ± 4.8 |  |
| F353L:T166I | 10.3 ± 3.5 | 14.8 ± 5.1 |  |

[a] Results similar to those published in Teschke (25).
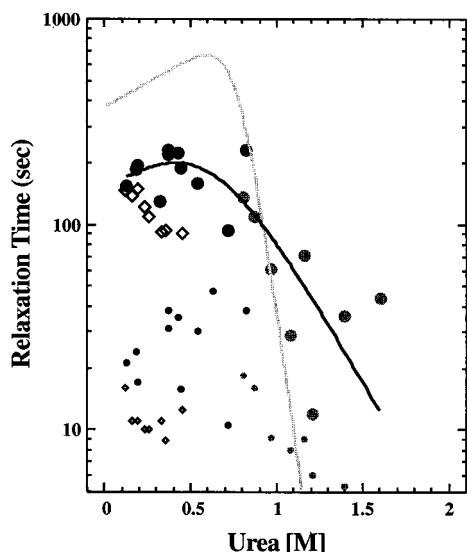


FIG. 4. **Urea dependence of the unfolding and refolding relaxation times as determined by CD.** Refolding reactions for S223F (*open diamonds*) and S223F:T166I (*black circles*) or unfolding reactions for S223F:T166I (*gray circles*) are shown at various urea concentrations. The *large symbols* are the slow kinetics, and the *small symbols* are the fast kinetics. The kinetic data were fit with a first order rate equation with two exponentials, and the relaxation time to reach equilibrium was determined. The relaxation times are plotted *versus* the urea concentration at which each experiment was performed. The *black line* is the fit of the slow relaxation times for S223F:T166I, as described under "Materials and Methods." The results of that fit are shown in Table III. Also shown is the fit of the slow folding and unfolding kinetics (*solid gray line*) of WT coat protein from Anderson and Teschke (21).

rived from the equilibrium experiments for the N ⇔ I transition. Furthermore, the midpoint of the S223F:T166I chevron (Fig. 4) corresponds with the midpoint of the N ⇔ I transition of the equilibrium curve for this mutant (Fig. 1). Taken together, these data are consistent with fitting the kinetic data with a two-state model for the N ⇔ I transition. The above data suggest that the *su* substitution decreases the rate of flickering from N ⇔ I, possibly aiding in the stabilization of the native state.

*The Suppressor Substitution Increases the Population of the Intermediate through Changes in the Rates of Folding and Unfolding*—Previous studies showed that mutant coat proteins carrying the *tsf* single amino acid substitutions have tryptophan fluorescence folding kinetics similar to WT coat protein, but faster unfolding kinetics (22). Here, we compare these folding and unfolding kinetics to determine if the suppressor substitution altered these rates when compared with the *tsf* parents.

To determine the rate of refolding, *tsf* or *tsf:su* coat proteins denatured in 6.75 M urea were diluted with buffered urea at various concentrations, and the re-equilibration was monitored by the intrinsic fluorescence of the six coat protein tryptophans (11). Each folding reaction was best fit by a first order reaction with two exponentials (data not shown), as observed for other

*tsf* coat proteins and WT coat protein (21, 22). For kinetic unfolding experiments, coat protein monomers were diluted with buffered urea solutions and monitored as above. The best fit for the unfolding kinetics was to a first order reaction with two exponentials (data not shown), as was previously observed for WT and other *tsf* coat proteins (21, 22).

The fast and slow relaxation times from the fit of the kinetic data obtained by tryptophan fluorescence, which primarily monitors the I ⇔ U transition, were plotted against the urea concentration in chevron plots (Fig. 5). The data were fit using a two-state model as previously described for several *tsf* coat protein mutants (22). We describe the fit of the chevron data for only the slow kinetics, because the scatter in relaxation times of the fast folding and unfolding reactions made the data difficult to fit. The scatter in all of our kinetic data is a result of the difficulty in fitting data from manual mixing experiments when one relaxation time is close to the dead time of mixing. The fit of the relaxation times for F353L coat protein from our previous work is also shown in Fig. 5 (22). The refolding and unfolding reactions for the *tsf:su* coat proteins diverge from two-state kinetics at urea concentrations near the peak of the chevron (*open gray* and *black circles*) as we have previously observed for the *tsf* mutant coat proteins (22). The data represented by these divergent points were also fit with a first order reaction with two exponentials (Fig. 6). Some of the data for these divergent points fit equally well to a first order reaction with a single exponential as with two exponentials. As the urea concentration approaches the apex of the chevron plot for the unfolding reactions, the total amplitude decreases causing the faster phase to be masked by a decrease in signal to noise. The amplitude for the faster phase of the two exponential fit was small, ~5% of the total amplitude. The slower phase, which had the majority of the amplitude, had similar relaxation times (±5%) whether the data were fit with one or two exponentials. We chose to fit all of the data with two exponentials because the rest of the chevron plot data, both unfolding and refolding reactions, were best fit with a first order reaction with two exponentials. We proposed previously that this divergence indicated a kinetic intermediate in the folding pathway of the *tsf* mutant coat proteins (22). As before, we fit the chevron plot data without these divergent points, a technique used by Korepanova et al. (42) for data similar to ours.

From the fits of the kinetic data, thermodynamic parameters were determined and are shown in Table IV. The stability (ΔG) and $m_{eq}$ calculated from the kinetic parameters were similar to the ΔG and m value determined by the equilibrium experiments for the I ⇔ U transition. In addition, the midpoint of each chevron (Fig. 5) corresponds with the midpoint of the I ⇔ U transition of the equilibrium curve for each mutant (Fig. 1), signifying that using a two-state model to fit the kinetic data was valid and consistent with our earlier work. The relaxation times for the refolding and unfolding reactions in the absence of denaturant were determined (Table IV). The addition of the suppressor substitution increased the rate of refolding to the intermediate 2-fold over the *tsf* parent coat protein and decreased the rate of unfolding between 2- and 7-fold compared with the *tsf* parent coat protein. These changes in rates likely stabilize the folding intermediate. Thus, the common mechanism of the suppressor substitution appears to be a decrease in the rate of unfolding, which stabilizes both the intermediate and native states.

## DISCUSSION

Single amino acid substitutions in bacteriophage P22 coat protein have been identified that cause a temperature-sensitive-folding (*tsf*) phenotype; these proteins fold properly and assemble into capsids when the infected cells are grown at low

TABLE III

*Kinetic parameters determined from analysis of the kinetic data in chevron plots monitored by circular dichroism*

Fits of the urea dependence of the slow relaxation times for folding and unfolding ($\tau$).

| | $\tau^{H_2O}$ folding | $\tau^{H_2O}$ unfolding | $\alpha$ | $m_{eq}$ | $\Delta G$ |
|---|---|---|---|---|---|
| | *s* | *s* | | *kcal/mol/M* | *kcal/mol* |
| WT[a] | 370 ± 20 | 4.6 ± 2.4 × 10⁶ | 0.93 ± 0.02 | −7.2 ± 1.2 | −5.6 ± 1.0 |
| S223F | ∼184 | Too fast for observation | | | |
| S223F:T166I | 155 ± 44 | 2400 ± 1300 | 0.68 ± 0.42 | −2.8 ± 0.7 | −1.6 ± 1.3 |

[a] WT data taken from Anderson and Teschke (21).
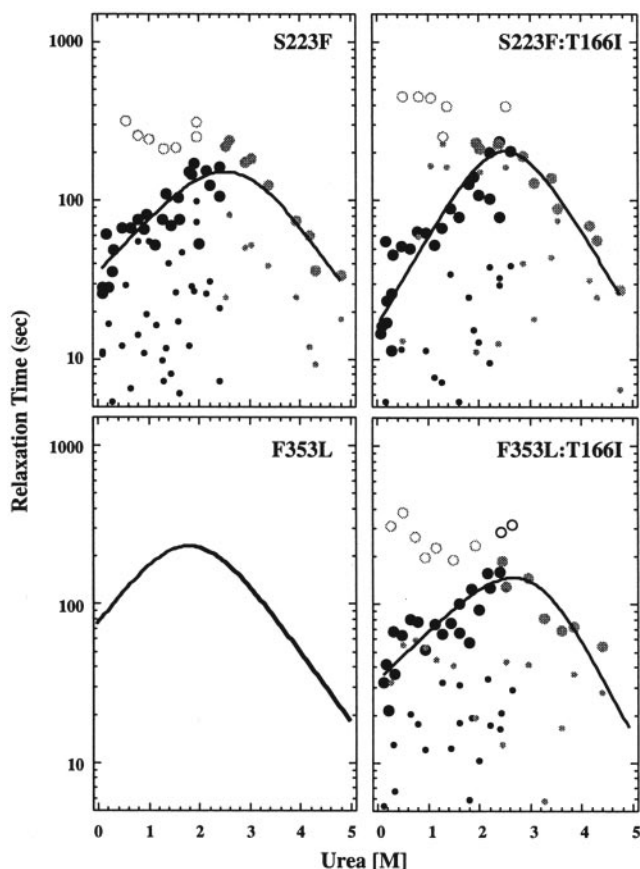


FIG. 5. **Urea dependence of the unfolding and refolding relaxation times monitored via tryptophan fluorescence.** Each of the *tsf* and *tsf:su* mutant coat proteins were refolded (*black symbols*) or unfolded (*gray symbols*) at various urea concentrations. The kinetic data were fit with a first order rate equation with two exponentials and the relaxation time to reach equilibrium was determined. The relaxation times are plotted *versus* the urea concentration at which each experiment was performed. The *large symbols* represent the slow kinetics, and the *small symbols* are the fast kinetics. The *open symbols* represent points diverging from the two-state model, and our treatment of these data is described under "Results." The *lines* are the fit of the slow relaxation times as described under "Materials and Methods." The results of those fits are shown in Table IV. The *F353L panel* shows the fit of the slow phase of the fluorescence data as determined in Doyle *et al.* (22).



FIG. 6. **Kinetic unfolding reaction at an intermediate urea concentration monitored by tryptophan fluorescence.** Coat protein monomers, prepared as described under "Materials and Methods," were rapidly diluted with buffered urea solutions at intermediate urea concentrations. This figure shows a representative unfolding experiment of F353L:T166I at 20 μg/ml in 1.92 M urea. The data in *Panel A* were fit with a first-order reaction with two exponentials. *Panel B* shows the residuals for this fit. *Panel C* shows the residuals for the fit to a first-order reaction with a single exponential. The relaxation times for the two exponential fit were 14.2 and 233.8 s, whereas the relaxation time for the single exponential fit was 231.0 s. The reduced $\chi^2$ improved by ∼10% for the two exponential fit over the single exponential fit.

temperatures, but at high temperatures, the *tsf* coat proteins misfold and aggregate (17, 18). The folding of the *tsf* coat proteins at high temperatures can be rescued by overexpression of GroEL and GroES (19, 20). Second amino acid substitutions have been isolated that suppress the *tsf* phenotype (*tsf:su*) and identify other positions of importance for coat protein folding (23, 24). Our previous studies showed that the *tsf:su* coat proteins do not increase the formation of productive phage by decreasing aggregation (24). Surprisingly, we found that the *su* substitution increases aggregation above the level of the *tsf* parent substitution. Instead, we identified an increase in the rate of subunit assembly into procapsids as the molecu-

lar mechanism for avoiding aggregation. In addition, the *tsf:su* coat proteins have enhanced interactions with GroEL and GroES *in vivo*.[2] Here, we have investigated the stability and kinetics of folding and unfolding of the *tsf* and *tsf:su* coat protein monomers to elucidate the mechanism by which the suppressor substitution compensates for the destabilizing effect of the *tsf* amino acid substitutions.

*The Effect of the tsf Substitutions on the Folding of Coat Protein*—Previously, we proposed that P22 coat protein has two folding domains defined spectroscopically: a tryptophan pocket that can be monitored by both tryptophan and bisANS fluorescence and a domain of secondary structure that can be monitored by CD at 222 nm (Fig. 7) (22). The destabilization caused by the *tsf* single amino acid substitutions primarily affects the domain of secondary structure, causing a rapid (sub-second) unfolding and refolding of that domain even in the absence of denaturant (Fig. 7, *red text*) (22). This rapid flickering from N ⇔ I caused the instability and the propensity to aggregate of the *tsf* coat proteins (22). Additionally, the rate of the unfolding reaction of the hydrophobic tryptophan pocket is increased ∼8- to 14-fold by the *tsf* amino acid substitutions leading to the destabilization of the intermediate, I₂ (Fig. 7, *red text*).

S223F coat protein was different than the other *tsf* mutant coat proteins in that it had observable CD refolding kinetics. Interestingly, the refolding kinetics increased in rate with in-

TABLE IV

*Kinetic parameters determined from analysis of the kinetic data in chevron plots monitored by tryptophan fluorescence*

Fits of the urea dependence of the slow relaxation times for folding and unfolding ($\tau$).

| | $\tau^{H2O}$ folding | $\tau^{H2O}$ unfolding | $\alpha$ | $m_{eq}$ | $\Delta G$ |
|---|---|---|---|---|---|
| | *s* | *s* | | *kcal/mol/M* | *kcal/mol* |
| WT[a] | $59 \pm 17$ | $39,000 \pm 11000$ | $0.73 \pm 0.12$ | $-1.4 \pm 0.3$ | $-3.8 \pm 1.2$ |
| S223F | $34 \pm 6$ | $5,000 \pm 700$ | $0.56 \pm 0.13$ | $-1.1 \pm 0.1$ | $-2.9 \pm 0.8$ |
| S223F:T166I | $16 \pm 6$ | $9,000 \pm 100$ | $0.49 \pm 0.11$ | $-1.5 \pm 0.1$ | $-3.8 \pm 0.6$ |
| F353L[b] | $76 \pm 11$ | $3,000 \pm 500$ | $0.51 \pm 0.11$ | $-1.2 \pm 0.1$ | $-2.2 \pm 0.3$ |
| F353L:T166I | $33 \pm 7$ | $22,000 \pm 1100$ | $0.67 \pm 0.12$ | $-1.3 \pm 0.3$ | $-3.8 \pm 1.1$ |

[a] WT data taken from Anderson and Teschke (21).
[b] F353L data taken from Doyle *et al.* (22).
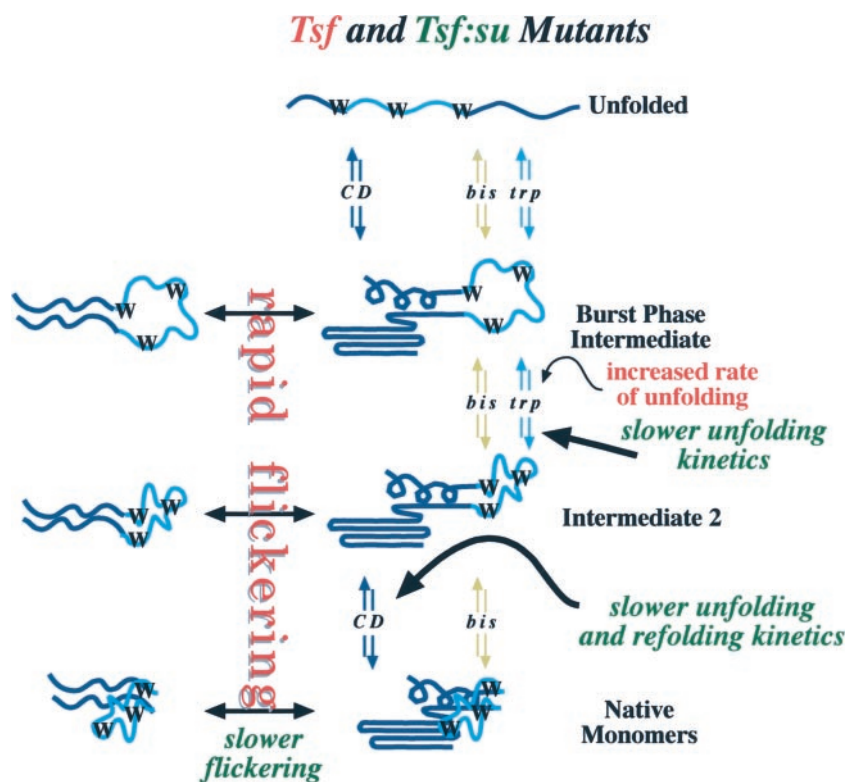


FIG. 7. **Model for suppression by the T166I substitution.** The model for the folding of *tsf* coat proteins (*red*) has been modified from Doyle *et al.* (22) to incorporate the *tsf:su* coat proteins (*green*). The model shows the two spectroscopically defined folding domains: the domain monitored by CD is in *dark blue*, and the domain monitored by tryptophan and bisANS fluorescence is in *light blue*. Coat protein has six tryptophans; the "W" letters in the model represent the hydrophobic patch in the protein to suggest the positions of the tryptophans. The *dark blue*, *light blue*, and *golden arrows* indicate steps followed by CD, tryptophan fluorescence, and bisANS fluorescence, respectively. The step monitored by CD for the *tsf* mutants occurs only in the burst phase of the folding reactions. The refolding step to native S223F is an exception, because the CD kinetics are observable but much faster than WT coat protein. The *su* substitution slows this step down, with observable unfolding kinetics for both *tsf:su* coat proteins and refolding kinetics for S223F:T166I. This change in the kinetics monitored by CD indicates a slower rate of flickering of the domain of secondary structure. In addition, the unfolding kinetics monitored by tryptophan fluorescence (for the $I_2 \Rightarrow U$ step) were significantly slower for the *tsf:su* coat proteins than their *tsf* parents, leading to an increased population of the intermediate. The final step in the folding pathway is the condensation of the two domains, which is monitored by bisANS. Folding kinetics monitored by bisANS fluorescence for the *tsf:su* coat proteins were like those for their *tsf* parents (data not shown), so no change is indicated.

creasing urea concentration. Similar kinetics had been observed for the $\alpha$-subunit of tryptophan synthase (34), dihydrofolate reductase (43), and ubiquitin (44, 45). There are two possible interpretations for this refolding phase: the presence of either an on-pathway or an off-pathway intermediate. In the case of an on-pathway intermediate, the equilibrium between populations of U and I are shifted toward U with increasing urea concentration, leading to a decrease in the population of the intermediate. Because relaxation times are the combination of the forward and the back rates of the reaction, the contribution of kinetics from the $I \Rightarrow U$ transition, which is faster in the presence of denaturant than the $U \Rightarrow I$ transition, makes the additive rate of refolding faster in denaturant. In the other scenario, an off-pathway intermediate acts as a trap that needs to be disrupted to resume productive folding. As the

denaturant concentration increases, the energy barrier between the trapped intermediate and the unfolded state becomes shallower, and therefore the rate of refolding increases. Although either explanation is possible, we favor the presence of an on-pathway intermediate because the stability ($\Delta G_{N \Leftrightarrow I}$) of the native state of S223F is so small that the native and intermediate states are virtually at the same energy level, where shifting between levels could easily occur. Although S223F coat protein had CD kinetics that were unusual for *tsf* mutant coat proteins, it followed the same trend observed previously for *tsf* coat proteins with an ~8-fold increase in the rate of unfolding of the intermediate, from $I \Rightarrow U$. This increase in the rate of unfolding of the *tsf* coat proteins appears to be the major factor in destabilization when compared with WT coat protein (21, 22).

*A Model for Suppression by the T166I Substitution*—Here we have studied the *tsf*:*su* coat proteins to find the mechanism of suppression by the T166I *su* substitution. For F353L:T166I coat protein, the *su* substitution stabilizes the folding intermediate. This increase in population is due to a 7-fold decrease in the rate of unfolding as monitored by tryptophan fluorescence, a probe primarily for the I ⇔ U transition (Fig. 7, *green text*). In addition, the rate of refolding for the U ⇔ I transition of F353L:T166I coat protein is two times faster than for F353L coat protein, indicating that the intermediate state will be more rapidly populated in the *su* mutant coat protein. The T166I substitution also increases the overall stability of F353L:T166I compared with F353L because of an increase in $\Delta G^0$ for the I ⇔ U transition. Additionally, unfolding kinetics examined by CD, which primarily monitors the N ⇔ I transition, are also observable for F353L:T166I coat protein, but not for F353L. This implies additional stability of the native state, likely due to a decrease in the rate of flickering of the domain of secondary structure. However, we do not see an increase in the stability of the native state indicating there must be a compensating change in the refolding rate, keeping the $\Delta G$ the same. The change in solvent-accessible surface area (*m* value) over the N ⇔ I transition was within error for F353L and F353L:T166I coat proteins. This indicated that the unfolding of native F353L:T166I coat protein to its intermediate exposed similar amounts of surface area to solvent as did F353L coat protein. The above data are consistent with the bisANS binding data, which shows the native state of F353L and F353L:T166I bind the same amount of bisANS with the same affinity.

When T166I is investigated in conjunction with S223F, the T166I substitution appears to affect the native state of S223F:T166I coat protein more dramatically than for F353L:T166I coat protein, with a smaller effect on the folding intermediate. However, the addition of the T166I substitution increases the stability of S223F:T166I coat protein. This increase in stability of the native state is likely due to the decrease in the rate of flickering of the domain of secondary structure, the N ⇔ I transition (Fig. 7, *green text*). Again, the bisANS binding data is consistent with the kinetic and thermodynamic data and suggests a stabilized native state for S223F:T166I coat protein.

Refolding kinetics are only observable for S223F and S223F:T166I coat proteins, whereas unfolding kinetics are observable for S223F:T166I as well as F353L:T166I coat protein. The relaxation time for refolding of S223F:T166I coat protein (I ⇒ N) in the absence of urea was 2-fold faster than for WT coat protein. In addition, the kinetics of unfolding for S223F:T166I coat protein (N ⇒ I) are much slower than for any other mutant coat protein, imparting stability to the native state, although they are 2000-fold faster than WT coat protein (21, 22). The stabilizing effect on the folding intermediate likely comes from a slower rate of unfolding of the hydrophobic pocket (I ⇒ U), as well as the faster rate of refolding from U ⇒ I. Overall, the suppressor substitution decreases the rate of unfolding of both the native and intermediate states, thereby increasing the stability and population of both states, but the effect on each state is dependent on the *tsf* parent substitution.

*The Stabilization of the tsf:su Coat Proteins Allows More Productive Interactions with a Chaperone Network*—The *su* substitution stabilizes both the intermediate and the native state for the *tsf* parent coat proteins, S223F and F353L. Aramli and Teschke (24) observed a greater degree of aggregation for the *tsf*:*su* coat proteins than for their *tsf* parents *in vitro*. The stabilization of the intermediate likely leads to the increased aggregation of the *tsf*:*su* coat proteins, and increased interactions with GroEL and GroES *in vivo*.[2] In agreement with the *in vitro* results presented here, our recent *in vivo* experiments

also show that not only is a higher percentage of *tsf*:*su* coat proteins bound to GroEL than their *tsf* parents, but the *tsf*:*su* coat proteins actually induce GroEL expression as compared with the induced GroEL levels for the *tsf* coat proteins. Thus, enhanced GroEL/ES interactions emerge as one function of the *su* substitution.

Aramli and Teschke (24) also determined that, in the presence of scaffolding protein, under conditions favorable for *in vitro* procapsid assembly, the *tsf*:*su* coat proteins assemble more efficiently than their *tsf* parents, decreasing overall aggregation. This result was consistent with our *in vivo* experiments, which showed that the interaction with scaffolding protein by the *tsf*:*su* coat proteins is essential for suppression of the *tsf* phenotype.[2] The *tsf*:*su* coat proteins require less scaffolding protein to make a procapsid than do their *tsf* parents, indicating that the *tsf*:*su* coat proteins have more favorable interactions with scaffolding protein. Moreover, the *tsf*:*su* coat proteins are able to produce procapsids at lower concentrations of scaffolding protein, as compared with their *tsf* parents, also suggesting that the *su* substitution causes enhanced interactions with scaffolding protein. This may be due to the increased stability of the *tsf*:*su* coat proteins imparted by a slower rate of flickering between the intermediate and the native state. We propose that this stabilization allows more time for interaction with scaffolding protein and favors assembly into procapsids over aggregation. Combined, the *su* substitutions appear to function through increased interactions with this chaperone network.

*Mechanisms of Global Suppression*—Two common modes of action have been determined for the global suppressors of other proteins: suppression of misfolding and aggregation by 1) improving folding or 2) increasing the stability of the protein. For β-lactamase and chloramphenicol acetyltransferase, the suppressor substitutions appear to suppress misfolding and aggregation without an increase in the stability of the protein (46, 47). Conversely, the global suppressor for the transmembrane receptor-like protein, human LAR, acts by increasing the stability of the native state of the protein through an increased efficiency of folding to the active state (48). The suppression mechanism of the *tsf* phenotype in bacteriophage P22 tailspike protein is dependent on the suppressor substitution. The *su* substitutions V331A and V331G stabilize both the native state and a thermolabile folding intermediate (49–52). In contrast, the *su* substitutions A334V and A334I destabilize the native state, due to steric strain, but improve a hydrophobic stack in a large β-helix stabilizing the folding intermediate (51–53).

In a manner similar to the P22 tailspike protein *su* substitutions V311A and V311G, the T166I *su* substitution in P22 coat protein stabilizes both a folding intermediate and the native state. The *su* substitution increases the population of the intermediate by slowing the rate of unfolding from I ⇒ U. GroEL can then interact with the intermediate to rescue it from aggregation. In addition, the *su* substitution increases the population of the native state, which augments the productive interactions with scaffolding protein increasing coat protein assembly into procapsids. This increase in population of the native state is in large part due to the decrease in the rate of flickering of a domain of secondary structure, between the intermediate and the native state. Consequently, we believe we have identified a mechanism for suppression of the *tsf* phenotype through changes in kinetics of folding and unfolding of an intermediate and the native state. The changes in kinetics work in concert with scaffolding protein, an assembly chaperone, and GroEL and GroES.

## REFERENCES

1. Anfinsen, C. B., and Haber, E. (1961) *J. Biol. Chem.* **236,** 1361–1363
2. Anfinsen, C. B. (1973) *Science* **181,** 223–230
3. Thomas, P. J., Qu, B.-H., and Pedersen, P. L. (1995) *Trends Biochem. Sci.* **20,** 456–459
4. Bonadio, J., Holbrook, K. A., Gelinas, R. E., Jacob, J., and Byers, P. H. (1985) *J. Biol. Chem.* **260,** 1734–1742
5. Liu, X., Kim, S., Dai, S., Brodsky, B., and Baum, J. (1998) *Biochemistry* **37,** 15528–15533
6. Chen, S., Ferrone, F. A., and Wetzel, R. (2002) *Proc. Natl. Acad. Sci. U. S. A.* **99,** 11884–11889
7. Bachinger, H. P., Morris, N. P., and Davis, J. M. (1993) *Am. J. Med. Genet.* **45,** 152–162
8. Milewski, M. I., Mickle, J. E., Forrest, J. K., Stanton, B. A., and Cutting, G. R. (2002) *J. Biol. Chem.* **277,** 34462–34470
9. Bhate, M., Wang, X., Baum, J., and Brodsky, B. (2002) *Biochemistry* **41,** 6539–6547
10. Botstein, D., Chan, R. K., and Waddell, C. H. (1972) *Virology* **49,** 268–282
11. Eppler, K., Wykoff, E., Goates, J., Parr, R., and Casjens, S. (1991) *Virology* **183,** 519–538
12. King, J., Lenk, E. V., and Botstein, D. (1973) *J. Mol. Biol.* **80,** 697–731
13. Fuller, M. T., and King, J. (1980) *Biophys. J.* **32,** 381–401
14. Prevelige, P. E., Jr., Thomas, D., and King, J. (1988) *J. Mol. Biol.* **202,** 743–757
15. King, J., and Casjens, S. (1974) *Nature* **251,** 112–119
16. Thuman-Commike, P. A., Greene, B., Jokana, J., Prasad, B. V. V., King, J., Prevelige, P. E., Jr., and Chiu, W. (1996) *J. Mol. Biol.* **260,** 85–98
17. Gordon, C. L., and King, J. (1993) *J. Biol. Chem.* **268,** 9358–9368
18. Gordon, C. L., and King, J. (1994) *Genetics* **136,** 427–438
19. Gordon, C. L., Sather, S. K., Casjens, S., and King, J. (1994) *J. Biol. Chem.* **269,** 27941–27951
20. Nakonechny, W. S., and Teschke, C. M. (1998) *J. Biol. Chem.* **273,** 27236–27244
21. Anderson, E., and Teschke, C. M. (2003) *Virology* **313,** 184–197
22. Doyle, S. M., Anderson, E., Zhu, D., Braswell, E. H., and Teschke, C. M. (2003) *J. Mol. Biol.* **332,** 937–951
23. Aramli, L. A., and Teschke, C. M. (1999) *J. Biol. Chem.* **274,** 22217–22224
24. Aramli, L., and Teschke, C. (2001) *J. Biol. Chem.* **276,** 25372–25377
25. Teschke, C. M. (1999) *Biochemistry* **38,** 2873–2881
26. Teschke, C. M., and King, J. (1993) *Biochemistry* **32,** 10839–10847
27. Galisteo, M. L., Gordon, C. L., and King, J. (1995) *J. Biol. Chem.* **270,** 16595–16601
28. Arakawa, T., and Timasheff, S. N. (1985) *Methods Enzymol.* **117,** 60–65
29. Laue, T. M., Shah, B. D., Ridgeway, T. M., and Pelletier, S. L. (1992) in *Analytical Ultracentrifugation in Biochemistry and Polymer Science* (Harding, S. E., Rowe, A. J., and Horton, J. G., eds) pp. 90–125, The Royal Society of Chemistry, Cambridge
30. Schuck, P. (2000) *Biophys. J.* **78,** 1606–1619
31. Finn, B. E., Chen, X., Jennings, P. A., Saal'au-Bethell, S. M., and Matthews, C. R. (1992) in *Protein Engineering: A Practical Approach* (Rees, A. R., Sternberg, M. J. E., and Wetzel, R., eds) pp. 168–189, Oxford University Press, Oxford
32. Schellman, J. A. (1978) *Biopolymers* **17,** 1305–1322
33. Zitzewitz, J. A., Bilsel, O., Luo, J., Jones, B. E., and Matthews, C. R. (1995) *Biochemistry* **34,** 12812–12819
34. Bilsel, O., Zitzewitz, J. A., Bowers, K. E., and Matthews, C. R. (1999) *Biochemistry* **38,** 1018–1029
35. Shi, L., Palleros, D. R., and Fink, A. L. (1994) *Biochemistry* **33,** 7536–7546
36. Secnik, J., Gelfand, C. A., and Jentoft, J. E. (1992) *Biochemistry* **31,** 2982–2988
37. Lakowicz, J. R. (1999) *Principles of Fluorescence Spectroscopy*, 2nd Ed., pp. 52–54, Kluwer Academic/Plenum Publishers, New York
38. Freidfelder, D. (1982) *Physical Biochemistry: Applications to Biochemistry and Molecular Biology*, 2nd Ed., pp. 662–664, W. H. Freeman and Co., San Francisco
39. Ghaemmaghami, S., Word, J. M., Burton, R. E., Richardson, J. S., and Oas, T. G. (1998) *Biochemistry* **37,** 9179–9185
40. Gloss, L. M., and Matthews, C. R. (1998) *Biochemistry* **37,** 15990–15999
41. Farris, F. J., Weber, G., Chiang, C. C., and Paul, I. C. (1978) *J. Am. Chem. Soc* **100,** 4469–4474
42. Korepanova, A., Douglas, C., Leyngold, I., and Logan, T. M. (2001) *Protein Sci.* **10,** 1905–1910
43. Jennings, P. A., Finn, B. E., Jones, B. E., and Matthews, C. R. (1993) *Biochemistry* **32,** 3783–3789
44. Roder, H., and Colon, W. (1997) *Curr. Opin. Struct. Biol.* **7,** 15–28
45. Khorasanizadeh, S., Peters, I. D., and Roder, H. (1996) *Nat. Struct. Biol.* **3,** 193–205
46. Sideraki, V., Huang, W., Palzkill, T., and Gilbert, H. F. (2001) *Proc. Natl. Acad. Sci. U. S. A.* **98,** 283–288
47. Van der Schueren, J., Robben, J., and Volckaert, G. (1998) *Protein Eng.* **11,** 1211–1217
48. Tsai, A. Y. M., Toh, M., Streuli, M., Thai, T., and Saito, H. (1991) *J. Biol. Chem.* **266,** 10534–10543
49. Danner, M., and Seckler, R. (1993) *Protein Sci.* **2,** 1869–1881
50. Chen, B., and King, J. (1991) *Biochemistry* **30,** 6260–6269
51. Beiβinger, M., Lee, S. C., Steinbacher, S., Reinemer, P., Huber, R., Yu, M.-H., and Seckler, R. (1995) *J. Mol. Biol.* **249,** 185–194
52. Schuler, B., and Seckler, R. (1998) *J. Mol. Biol.* **281,** 227–234
53. Miller, S., Schuler, B., and Seckler, R. (1998) *Protein Sci.* **7,** 2223–2232